

Anisotropy and orientational dependence of magnetization reversal processes in epitaxial ferromagnetic thin films

C. Daboo, R. J. Hicken, E. Gu, M. Gester, S. J. Gray, D. E. P. Eley, E. Ahmad, and J. A. C. Bland
Cavendish Laboratory, University of Cambridge, Madingley Road, Cambridge CB3 0HE, United Kingdom

R. Ploessl and J. N. Chapman

Department of Physics and Astronomy, University of Glasgow, Glasgow G12 8QQ, United Kingdom

(Received 27 October 1994; revised manuscript received 9 March 1995)

We have undertaken a detailed study of the macroscopic and microscopic magnetization reversal processes in epitaxial ferromagnetic thin films with varying cubic and uniaxial magnetocrystalline anisotropy strengths. The macroscopic magnetization reversal processes were observed with in-plane magneto-optic Kerr effect (MOKE) vector magnetometry as a function of the relative anisotropy strengths and on the orientation of the applied field with respect to the anisotropy directions. Measurements of the component of magnetization in the plane of the sample and perpendicular to the applied field allow a precise determination of the relative orientation of the hard and easy in-plane anisotropy axes. This can be used to accurately determine the ratio of uniaxial to cubic anisotropy constants, when the ratio is less than one. The ratios obtained from MOKE agree well with those obtained by Brillouin light scattering (BLS). MOKE vector magnetometry reveals loop features that can be associated with either one or two irreversible jumps in the direction of the magnetization, depending sensitively on the anisotropy ratio and the orientation of the applied field. Minimum-energy calculations predict that the reversal process should proceed by a continuous rotation of the magnetization vector with either one or two irreversible jumps between single-domain states, depending on the applied field orientation and the nature of the anisotropy of the film. The calculations provide a good qualitative description of the observed reversal process, although the magnetic microstructure influences the exact values of the switching fields. Sequences of Lorentz microscopy images were made in the vicinity of the two switching fields to reveal the microscopic reversal mechanism. These images provide direct evidence that the reversal proceeds by domain-wall motion between single domain states. In the case where the applied field is oriented away from the easy axis direction, a single domain intermediate state is observed during magnetization reversal, as suggested by the MOKE measurements and predicted by the calculations. In addition, the reversal mechanism with the field applied close to an easy axis reveals that the single jump observed in the MOKE loops actually corresponds to a two-step process on a microscopic scale.

I. INTRODUCTION

In previous studies of the Fe/GaAs(001) system¹⁻⁵ the magnetization reversal process was shown to be sensitive to the overall anisotropy and orientation of the magnetic field with respect to the crystallographic axes. These studies did not fully explore the dependence of the reversal mechanism on the exact ratio r of uniaxial to cubic anisotropy constants ($r = K_u/K_1$). In addition, the micromagnetic mechanisms by which reversal proceeded were only postulated,² and not shown experimentally. Here we extend these studies to show how the detailed macroscopic switching behavior is expected to vary with precise orientation of the applied field and the exact ratio r of uniaxial to cubic anisotropy constants, which are known to be present in such samples.⁴ By studying the switching behavior over a wide range of anisotropy values we have also been able to distinguish two different two-jump switching mechanisms, not previously discussed. In addition, Lorentz microscopy in an applied field⁶ has been used to image the domains in our films during the magnetization reversal process. Using such

images, we are now able to explain how the switching develops via the domain structure in applied fields, and to see the differences between the one-jump and two-jump reversal processes.

We are also able to show that, when the sample orientation relative to field is accurately controlled with high-precision rotary stepper motors, an accurate determination can be made of the relative orientations of the hard and easy anisotropy axes, and thus the ratio r of uniaxial to cubic anisotropy strengths in the sample, using the magneto-optic Kerr effect (MOKE).

The studies presented here are important in understanding the role of anisotropies during the magnetization reversal process in single layers. This work is also needed to understand the magnetization reversal in multilayer systems where the effects of interlayer exchange coupling and anisotropy need to be separated. This knowledge could extend the scope for potential device applications of such systems.

The Fe/GaAs(001) system, for which the magnetic and structural properties have been extensively studied, has a number of advantages when studying the generic switching behavior of epitaxial thin films. In particular, the

demagnetizing fields of such films constrain the magnetization to the film plane, simplifying the analysis. Also, the single-crystal nature of such films provides well-defined anisotropies. One of the features of the Fe/GaAs(001) system is the observed thickness-dependent anisotropy behavior,^{4,7} which provides a means of systematically producing samples with a range of anisotropy behavior for our switching studies. Similar thickness-dependent uniaxial anisotropy has also been observed in the Fe/GaAs(110) system,⁷⁻⁹ though in this case the symmetry of the (110) substrate orientation produces a two-step switching behavior which varies with the angle of the applied field in the plane of the sample. The Fe/GaAs(001) system also provides films of sufficient quality to clearly observe an almost single-domain behavior and a domain structure not limited by defects.⁶ This allows a simple analysis of the magnetization reversal mechanism in terms of the standard coherent-rotation model.¹⁰

In agreement with previous results,^{2,3} we find that the macroscopic magnetization reversal as observed by MOKE occurs by either one or two irreversible jumps. These jumps occur at distinct switching fields depending on the ratio of the anisotropies r and the orientation of the applied field. This switching behavior can be determined by measuring MOKE loops for both the component of magnetization parallel to the applied field (M_{\parallel}) and the component of magnetization perpendicular to the applied field (M_{\perp}) but in the plane of the sample.^{1,11} This MOKE vector magnetometry technique¹¹ has proved powerful in determining the detailed switching features of epitaxial thin-film and multilayer samples. Our choice of MOKE geometries for measuring the magnetization components together with the Lorentz microscopy measurements allow us to confirm that the jumps occur between almost single-domain states. The Lorentz microscopy images also reveal trends in the orientation of the domain walls and the reorientation of the domain structure according to the applied field during the switching process.

II. EXPERIMENT

The Fe samples were grown under UHV conditions (pressure during evaporation less than $\sim 5 \times 10^{-10}$ mbar) on GaAs(001) substrates and studied by low-energy electron diffraction (LEED), Auger spectroscopy, and *in situ* MOKE. The substrates were held at 150°C during Fe growth at $\sim 1 \text{ \AA min}^{-1}$ from the *e*-beam evaporator. A series of samples with thickness between 30 and 450 Å were grown, together with a wedge-shaped Fe-film of thickness range 10–60 Å. Each was capped with $\sim 20 \text{ \AA}$ of Cr, which from electron energy-loss spectroscopy (EELS) measurements¹² was found to be sufficient to prevent oxidation of the Fe layer. *In situ* MOKE was used to study the evolution of the magnetic anisotropy as the Fe films were grown⁷ so that films with different final anisotropy strengths could be produced.

The fixed-thickness samples were characterized *ex situ* using Brillouin light scattering (BLS) in order to determine the anisotropy constants K_1 and K_u of each sample. By fitting the BLS data as a function of the angle ϕ be-

tween the applied field direction in the plane of the sample and the hard uniaxial anisotropy axis it was possible to determine the quantities $2K_1/M$ and $2K_u/M$.¹³ The thickness dependence of the anisotropy is reported elsewhere,⁷ but in general it was found that thinner Fe layers had a larger anisotropy ratio r , and a reduced average magnetization.

It is important to understand the relative orientations of the uniaxial and cubic anisotropies in these films as this affects the magnetization reversal behavior. The uniaxial anisotropy in these films is always found to be parallel to the $\langle 110 \rangle$ directions with the in-plane hard direction along $[110]$ and the in-plane easy direction along $[1\bar{1}0]$,^{4,7} as illustrated in Fig. 1(a). The fixed absolute orientation of the uniaxial anisotropy is related to the directions of the reconstructed surface of the underlying GaAs substrate.⁷ The cubic anisotropy has in-plane hard directions along $\langle 110 \rangle$ and in-plane easy directions along $\langle 100 \rangle$ as illustrated in Fig. 1(b). As a result, in samples which have both uniaxial and cubic anisotropies the two in-plane $\langle 110 \rangle$ directions are inequivalent since the $[110]$ axis is a combination of a hard cubic direction and the hard uniaxial direction (the hard-hard axis) while the $[1\bar{1}0]$ axis is a combination of a hard cubic direction and the easy uniaxial direction (the hard-easy axis) as shown

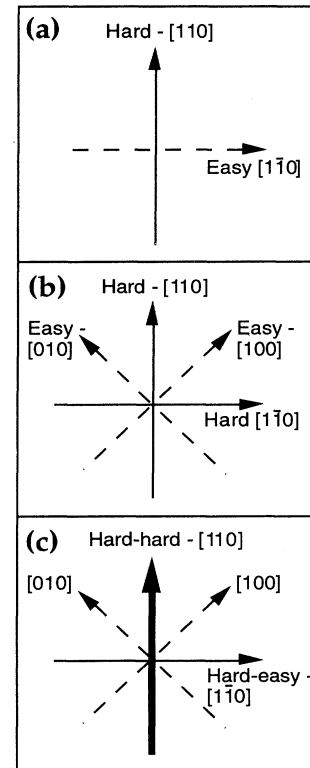


FIG. 1. The direction of anisotropy axes relative to the crystallographic axes in Fe/GaAs(001) films: (a) uniaxial anisotropy; (b) cubic anisotropy; (c) mixture of uniaxial and cubic anisotropies.

in Fig. 1(c). As a result, it is energetically more favorable for the magnetization to jump over the hard-easy axis than over the hard-hard axis and this has a significant bearing on the reversal process. Also the position of the overall easy direction in the samples depends on the ratio of the uniaxial to cubic anisotropies r , and changes from the $[1\bar{1}0]$ direction to a $\langle 100 \rangle$ direction as r varies from unity to zero. A simple expression for the angle θ between the hard-hard axis and the easy axis can be evaluated from the magnetostatic energy equation,¹⁴ and is given by

$$\begin{aligned} \cos 2\theta &= -r \quad \text{for } |r| \leq 1, \\ \theta &= 90^\circ \quad \text{for } |r| \geq 1. \end{aligned} \quad (1)$$

Thus the position of the easy axes can provide a useful measure of the anisotropy ratio r when $|r| \leq 1$.

III. VECTOR MAGNETOMETRY TECHNIQUE

The MOKE vector magnetometry technique used here measures M - H MOKE loops for two orientations of the applied field in the plane of the sample, parallel (M_{\parallel}) and perpendicular (M_{\perp}) to the plane of incidence of the light. This produces an M_{\parallel} - H and an M_{\perp} - H MOKE loop which can be used to determine the orientation and relative strength M/M_s (where M_s is the saturation magnetization) of the average magnetization as sampled over the area of the laser beam. In our case we use the same optical geometry for measuring M_{\parallel} - H and M_{\perp} - H MOKE loops so that it was possible to determine M_{\parallel}/M_s and M_{\perp}/M_s directly from the resulting loops^{11,15} without the need for additional scaling.

To conduct these measurements the sample and an electromagnet were separately mounted on two concentric precision (0.001° step) rotary stepper drives, so that they could each be turned independently to any desired orientation over the full 0° - 360° range under computer control. In addition, a linear motion stage was attached to the sample rotary stage to provide a precise ($1 \mu\text{m}$ step) linear translation of the sample so that wedge-shaped films could be easily studied as a function of position and therefore film thickness along the wedge. The sample was mounted on a two-axis tilt (mirror) mount so that it could be adjusted in such a way that the sample normal and axis of rotation of the rotary stage were parallel. This ensures that as the sample is rotated the reflected beam remains fixed and aligned with the detection optics. In addition, the incident laser beam was positioned so that it was incident on the sample at its center of rotation, so that the beam always illuminated the same part of the sample to within one beam diameter ($\sim 1 \text{ mm}$) as the sample was rotated. For the wedge-shaped film the laser beam was focused onto the sample to give a spot size of $\sim 0.2 \text{ mm}$ to minimize the spread in film thickness sampled by the laser beam. In this case the beam could only be aligned to a precision of $\sim 0.5 \text{ mm}$ so that as the sample was rotated the beam could sweep out a circle of radius up to $\sim 0.5 \text{ mm}$, limiting the accuracy of the thickness range sampled by the beam. For our wedge-shaped sample with a thickness range of 50 \AA over a dis-

tance of 15 mm , this corresponds to an accuracy of $\pm 0.85 \text{ \AA}$, and is less than the accuracy to which the absolute thicknesses are known from growth.

The importance of using high-precision rotary stepper drives can be emphasized by looking at the M_{\perp} - H loop in the vicinity of a hard axis for a typical sample. Figure 2 shows a series of loops taken for sample orientations around the hard-hard axis ($\phi \approx 0^\circ$) at 0.001° resolution. A "collapse" in the loop is clearly observed as the sense of the magnetization rotation reverses when the direction of the hard axis is crossed. This "collapse," which is to be expected for any real films in some angular range, could be due to a number of different possibilities. One possibility is that there will be small pinning centers in the film, each pinned to one side or other of the hard-axis direction. This will induce domains with orientations either side of the hard axis, depending on the precise orientation of the applied field, giving rise to a spread in domain orientations. Thus when the field is applied in a

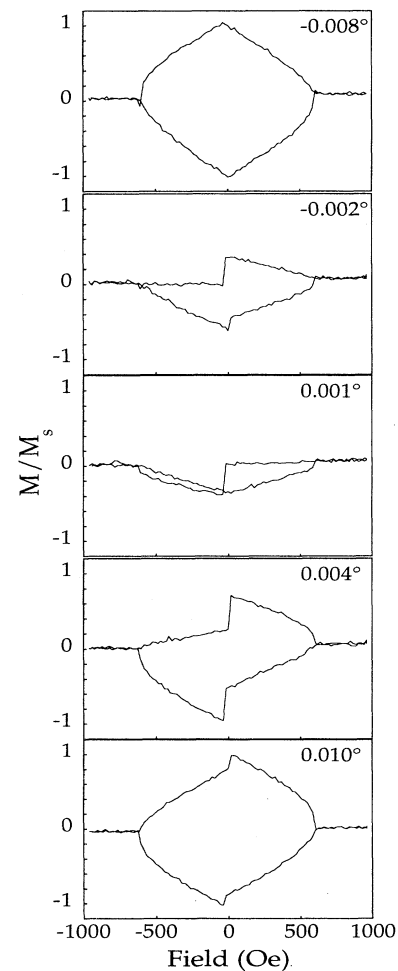


FIG. 2. The "collapse" of MOKE loops taken for applied field directions in the plane of the Fe/GaAs(001) sample close to the hard-axis direction.

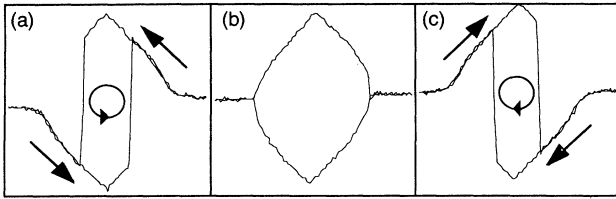


FIG. 3. M_1 - H MOKE loops taken with the applied field close to the direction of the hard axis to show the change in the sense of the loops as the hard-axis direction is traversed. The angles from the hard axis (determined by the collapse in the loop) were (a) $+0.5^\circ$, (b) $+0.05^\circ$, and (c) -0.5° .

direction within the angular range of the spread in domain orientations, some domains will rotate one way while others rotate in the opposite sense as the field is reversed. This results in the average magnetization of the film as detected by MOKE reducing to zero as the direction of the average hard axis is approached. Alternatively any inhomogeneities in the field or the anisotropies across the film will result in the same behavior. This effect is unlikely to be associated with a mosaic spread in crystallographic directions which would cause a ripple, since in this case only a perturbation in the direction of the magnetization occurs in contrast to the complete "collapse" we see.

M_1 - H MOKE loops can be used to determine precisely the location of the hard and easy in-plane anisotropy axes. When the applied field direction is close to a hard or easy axis, the magnetization vector moves, respectively, away from or towards the axis as the field is reduced as favored by the magnetostatic energy. Therefore, depending on which side of the anisotropy axis the field is applied, the magnetization will rotate in plane in either a clockwise or anticlockwise sense. A change in the clockwise or anticlockwise motion of the magnetization can be clearly seen in perpendicular-component M_1 - H MOKE loops (see Fig. 3) and, by using high-precision rotary stepper drives to turn the sample and align the magnet, it is possible to accurately determine the angles of the hard and easy axes in the sample plane. In general, this can be done to an accuracy of better than 0.01° for the hard axes and $\sim 0.1^\circ$ for the easy axes. Therefore using Eq. (1) it is possible to determine the anisotropy ratio r to great accuracy when $|r| < 1$ from the relative orientation of the hard-hard and easy axes. Note that a sense change cannot be determined from parallel-component $M_{||}$ - H MOKE loops, illustrating the importance of measuring M_1 - H MOKE loops as well.

IV. RESULTS

A. Experimental switching behavior—MOKE

In general it was found from MOKE vector magnetometry that the magnitude of the magnetization vector remained virtually constant during the reversal process,

indicating that the sample behaved almost as a single domain, except very close to a switching field value. At these critical fields the samples have been observed by Lorentz microscopy to switch via domain-wall motion as described elsewhere.⁶ The Lorentz microscopy results also confirm that an almost single-domain coherent-rotation process occurs away from the switching field regions.

The top panels in Figs. 4, 5, and 6 show three typical sets of $M_{||}$ - H and M_1 - H MOKE loops illustrating the different switching behavior observed in our samples according to thickness and thus anisotropy ratio. These loops were taken from the wedge-shaped Fe film for an anisotropy ratio $r = 0.4 \pm 0.02$ and for various angles ϕ of the applied field with respect to the in-plane hard-hard anisotropy axis. In Fig. 4 ($\phi = 75^\circ$) both loops show one irreversible jump at the same field of ~ 50 Oe as the field is reversed, corresponding to "one-jump" switching. In Fig. 5 ($\phi = 20^\circ$) both loops show two irreversible jumps as the field is reversed, corresponding to "two-jump" switching. Each of these two jumps occurs when the magnetization traverses one of the two hard-axis directions that exist in a sample with $|r| < 1$. In the case of Fig. 6 ($\phi = 60^\circ$) a "reversed" two-jump switch occurs since the magnetization initially rotates away from the field direction in a clockwise sense, say, but switches back over the field direction in an anticlockwise sense.

The observed results for $M_{||}$ and M_1 can be used to

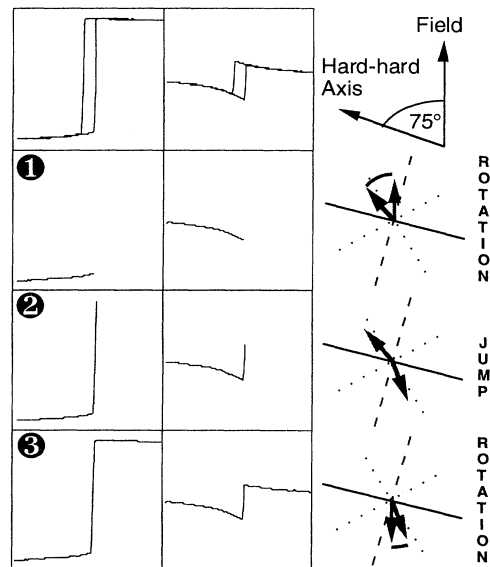


FIG. 4. The one-jump reversal sequence of the magnetization vector (right-hand column) compared to the corresponding sections of the MOKE loop (left-hand column). The initial (gray arrow) and final (black arrow) orientations of the magnetization are shown for each corresponding section of the MOKE loop. The hard-hard axis is shown as a solid line, the hard-easy axis as a long-dashed line, the easy axes are shown as dotted lines, and the direction of the applied field is taken as vertical.

determine the orientation of the magnetization in the plane of the film as the reversal process proceeds as illustrated by the additional panels in Figs. 4, 5, and 6. For the one-jump case shown in Fig. 4, the left-hand column of plots shows each stage of the M_{\parallel} - H hysteresis loop as it develops, the center column shows each stage of the M_{\perp} - H hysteresis loop as it develops, while the right-hand column shows how the orientation of the magnetization changes with respect to the sample's crystallographic axes during that stage of the loop; the top panel shows the whole loop. The solid axis in the right-hand column plots indicates the direction of the sample's hard-hard anisotropy axis, the long-dashed lines represent the sample's hard-easy axis, while the dotted lines correspond to the directions of the easy anisotropy axes. The gray arrow represents the positions of the magnetization at the start of the loop segment, while the solid arrow shows the position of the magnetization at the end of the loop segment. The applied field direction is taken to be vertical in each figure.

In stage 1 the magnetization undergoes a coherent-rotation process, moving away from the direction of the

applied field and away from the nearest hard anisotropy axis and towards the nearest easy anisotropy axis. In stage 2 the magnetization undergoes an irreversible jump over both hard axes and over the direction of the applied field. This is followed by stage 3 in which it undergoes coherent rotation towards the direction of the reversed applied field. Thus only a single jump occurs during this reversal process.

Figure 5 shows the two-jump process in a similar manner to Fig. 4. In this case there are five stages to the reversal. Stage 1 is again a coherent rotation of the magnetization away from the field direction and away from the nearest hard axis (in this case the hard-hard axis). Stage 2 corresponds to an irreversible jump over a single hard anisotropy axis (in this case the hard-easy axis which it is energetically more favorable for the magnetization to cross), but unlike the one-jump process the magnetization does not jump over the direction of the applied field (i.e., only one hard axis is crossed). This means that there is the hard-hard anisotropy axis between the magnetization and the direction of the reversed applied field. As a result a second jump is required after the

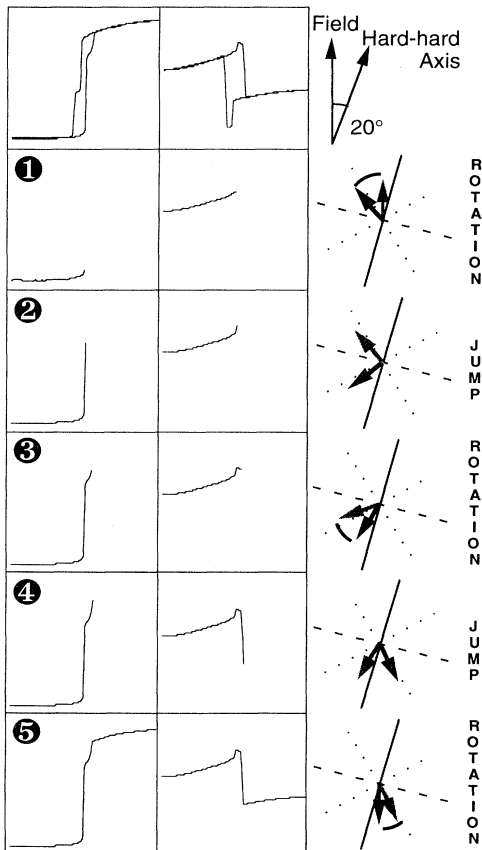


FIG. 5. The two-jump reversal sequence of the magnetization vector (see caption for Fig. 4 for full description).

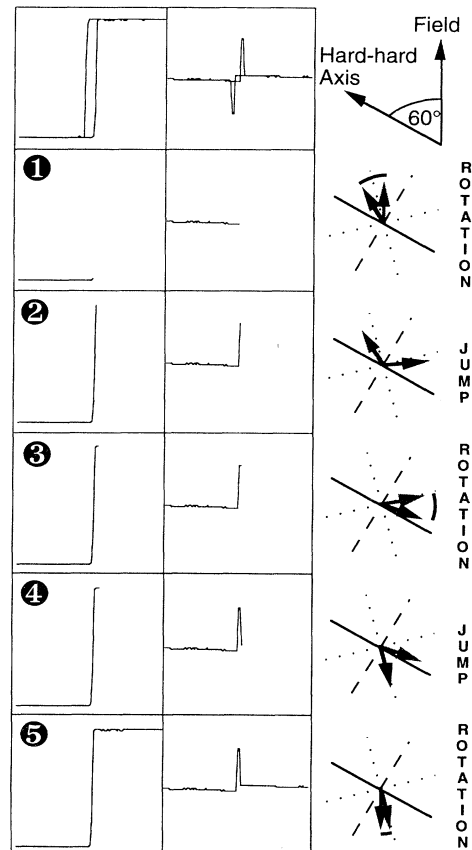


FIG. 6. The "reverse" two-jump reversal sequence of the magnetization vector (see caption for Fig. 4 for full description).

coherent-rotation process of stage 3. This second jump, stage 4, results in the magnetization jumping over the hard-hard axis and the reversed applied field direction, and it finally undergoes coherent rotation in stage 5 to lie in the direction of the reversed applied field. This results in a two-jump process, where two distinct switching fields can be observed in the MOKE M - H loops. One important point about this mechanism is that it requires two distinct hard axes in the plane of the sample. This condition only arises when the ratio of uniaxial to cubic anisotropies r is less than unity. Thus when the uniaxial anisotropy is stronger than the cubic anisotropy only a one-jump process can occur, and this is indeed observed to be the case as shown later.

Figure 6 illustrates the "reversed" two-jump process. Here, the direction of the applied field lies between the hard-easy axis direction and an easy anisotropy axis direction. In this case stage 1 again consists of a coherent rotation away from the direction of the applied field and away from the hard-easy axis direction. However, in stage 2, the magnetization jumps back over the direction of the applied field and over the hard-easy axis—a process which is energetically more favorable than jumping over the hard-hard axis for the particular initial conditions chosen. Stages 3, 4, and 5 are again coherent rotation, an irreversible jump (over the hard-hard axis), and the final coherent rotation, respectively. This defines the "reverse" two-jump switch in which the magnetization makes its first jump in the opposite direction to which it initially rotates in stage 1.

B. Modeling of macroscopic switching behavior

In order to study the magnetic switching behavior in more detail we used a coherent-rotation model^{10,14} to calculate the shape of the M_{\parallel} - H and M_{\perp} - H loops, for various values of the in-plane azimuth angle ϕ and the anisotropy ratio r . The calculations verified that the reversal process can proceed by either one or two jumps depending on the exact values of ϕ and r . The different switching regimes can be understood from the calculated switching behavior by tracking local energy minima as a function of applied field strength. Figure 7 shows the calculated track of energy minima as a function of applied field strength (horizontal axis) and orientation γ of the magnetization relative to the applied field direction for positive saturation (vertical axis) for three different jump processes. In each case the field is applied along one of the cubic easy axes. For these calculations the sum of the cubic and uniaxial anisotropies was kept constant at the value of the bulk cubic anisotropy of Fe, $K_1 + K_u = K_{1 \text{ bulk}} = 0.45 \times 10^6 \text{ erg cm}^{-3}$, but their ratio r was chosen to provide an illustration of the different switching behavior that can be observed. Three values of r were used: $r = 3.5$ [Fig. 7(a)—one jump]; $r = 0.5$ [Fig. 7(b)—two jump]; and $r = 0$ [Fig. 7(c)—"nonideal" two jump]. The bulk value of the magnetization for Fe, $M = 1.71 \times 10^{-3} \text{ emu cm}^{-3}$, was used and the film was taken to have a thickness of 20 Å. The thickness has no direct bearing on the simulated switching behavior, though it does affect the observed switching behavior as a

result of the thickness dependence of the anisotropies.

Figure 7(a) illustrates the one-jump process: the reversal process starts off with the magnetization in the negative saturation energy minimum with orientation close to the applied field direction $\gamma \approx 180^\circ$. As the field reverses this minimum rotates away from the field direction and becomes shallower, eventually disappearing at the coercive field H_c . At this point the magnetization undergoes an irreversible jump (as indicated by the arrow) and falls into a different energy minimum. In the one-jump switching process this second minimum is the positive saturation energy minimum, and the magnetization rotates back toward the direction of the applied field as it is taken towards positive saturation at $\gamma \approx 0^\circ$.

In the two-jump switching process illustrated in Fig. 7(b), there are additional energy minima that exist when the negative saturation minimum disappears at $H = H_{c2}$, with the result that the magnetization falls into an intermediate minimum in preference to the positive saturation minimum. However, as the field is further reversed this

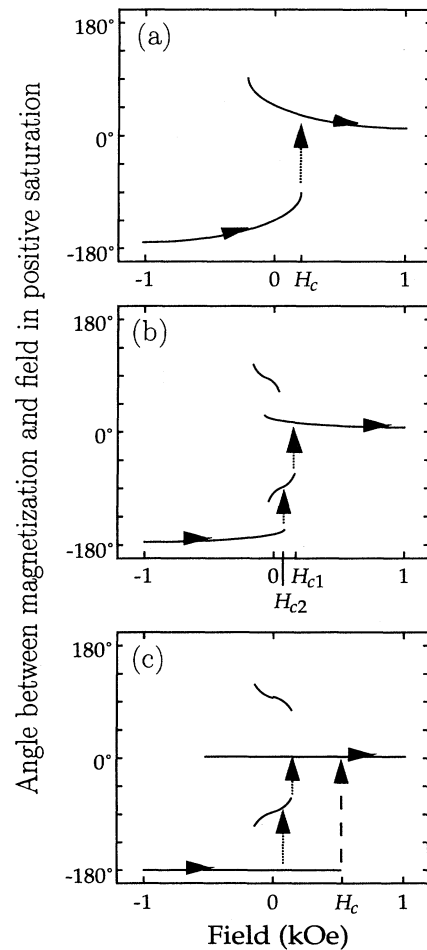


FIG. 7. The track of energy minima as a function of applied field (horizontal axis) and magnetization orientation (vertical axis): (a) one-jump process; (b) two-jump process; (c) defect-induced two-jump process.

intermediate minimum also disappears at $H = H_{c1}$ and the magnetization eventually ends up in the positive saturation energy minimum.

The two processes described above can be regarded as “ideal,” that is, the magnetization remains in an energy minimum until it disappears. In reality, defects such as strongly pinned reverse domains or nucleation sites induce domain-wall sweeping and nucleation which will cause the magnetization to jump earlier than the fields predicted by the coherent-rotation model. Figure 7(c) illustrates one possible “nonideal” case. Here intermediate minima are present as in the case illustrated by Fig. 7(b), but they disappear before the negative saturation minimum disappears at $H = H_c$. In the “ideal” case this would result in a one-jump process as the magnetization would jump directly from the negative saturation minimum to the positive saturation minimum at $H = H_c$. However, in this “nonideal” case, the magnetization jumps *before* the negative saturation minimum has disappeared, and *before* the intermediate minima have disappeared, with the result that a two-jump switch occurs when the calculations predict a one-jump switch. This type of “nonideal” behavior is indeed observed in our samples.

C. Macroscopic switching phase diagram

It is possible to use the coherent-rotation model to predict the type of switching behavior that should be expected for “ideal” samples as a function of the direction of the applied field ϕ with respect to the crystallographic axes of the sample and the anisotropy ratio r . The boundary between the one- and two-jump switching regimes can be defined as the point at which the intermediate and negative saturation minima both disappear at the same applied field. Thus a phase diagram can be produced which summarizes the one- and two-jump processes as a function of ϕ and r . Experimental data can then be compared with this phase diagram to determine how good the coherent-rotation model is at predicting the switching mechanism.

The phase diagram of the switching behavior is shown in Fig. 2 of Ref. 5. Experimental results for three samples with anisotropy ratios of ~ 0 (sample 1—almost completely cubic), 0.4, 0.6, 0.8, 1.1 (sample 2—various positions along the wedge-shaped sample), and 1.8 (sample 3—strongly uniaxial) are also shown at 5° intervals with different symbols to indicate different switching behavior. The anisotropy ratios were determined from a combination of MOKE and BLS. When $|r| < 1$ MOKE measurements of the angle θ between the hard-hard axis and the easy axis were used to determine r according to Eq. (1), and these agreed well with values of r determined by BLS. Only BLS could be used when $|r| > 1$ for determining the anisotropy ratio.

For $|r| > 1$ the calculations show that only one-jump switching can occur, and this is confirmed by the experimental results for sample 3 (with $r = 1.8$) and sample 2 (with $r = 1.1$). The results for sample 2 (with $r = 0.4, 0.6$, and 0.8) are in good agreement with the calculations, though close to the easy axis it is difficult to discriminate

between one- and two-jump switching because it is difficult to discriminate between an irreversible jump process and a rapid rotation of the magnetization on a macroscopic scale. Reverse two-jump loops are only seen on the hard-easy axis side of the easy axis, as expected. For sample 1 (with $r = 0$), the observed switching behavior conflicts with that predicted by the calculations since two-jump switching is always present, indicating that domain-wall sweeping can be more easily induced when r is close to zero.

The values of the two-jump switching fields H_{c1} and H_{c2} are seen to depend on the direction of the applied field ϕ in the plane of the sample. The observed dependence of H_{c1} and H_{c2} on the direction of the applied field⁵ is similar to that reported elsewhere.²

D. Microscopic switching behavior—Lorentz microscopy

To gain insight into the microscopic magnetic switching behavior described in the preceding sections, the micromagnetic domain structure and domain evolution in an Fe(35 Å)/GaAs(001) film with $r = 0.16$ were studied by a Lorentz transmission electron microscope (TEM) equipped with a magnetizing stage.¹⁶ After mounting on the magnetizing stage, the thin-film specimens can be rotated about a vertical axis in the microscope by an external drive so that the field can be applied at any in-plane direction with respect to the specimen’s crystallographic axes.

As an example of the Lorentz microscopy measurements we present results for the magnetization reversal observed with the applied field close to a hard axis where two-jump switching is observed in the MOKE loops. Though both hard-axis directions were studied, we saw little qualitative difference between the microscopic reversal processes between the two directions, therefore we present the results for reversal close to the [110] hard-hard axis direction only. First a single-domain state was induced by applying a magnetic field (H_i) in the microscopic close to the [110] hard-hard axis direction as determined from the diffraction pattern. Then the field was reduced to zero. In this remanent state, no domain walls were observed, indicating that the Fe film was still in a single-domain state. Magnetization reversal was then studied by applying successively greater fields parallel to $[\bar{1}\bar{1}0]$. The single-domain state broke up when the reverse field (H_r) was increased to the first critical strength (H_{c2} as observed in the MOKE loops) at which domain walls were first observed. A Fresnel image recorded at $1.7H_{c2}$ field strength is shown in Fig. 8 as an example. In this image, the domain walls appearing as bright and dark narrow bands can be seen clearly. It should be noted that most dark lines and bands shown in the image are bend contours coming from the single-crystal GaAs substrate. Minor tilting of the specimen allows these to be distinguished unambiguously from the magnetic contrast of interest. As the reverse field strength increased from H_{c2} , the evolution of domain structures and magnetization distributions are interpreted from Fresnel images similar to Fig. 8 and these are shown schematically in Figs. 9(a) to 9(m).

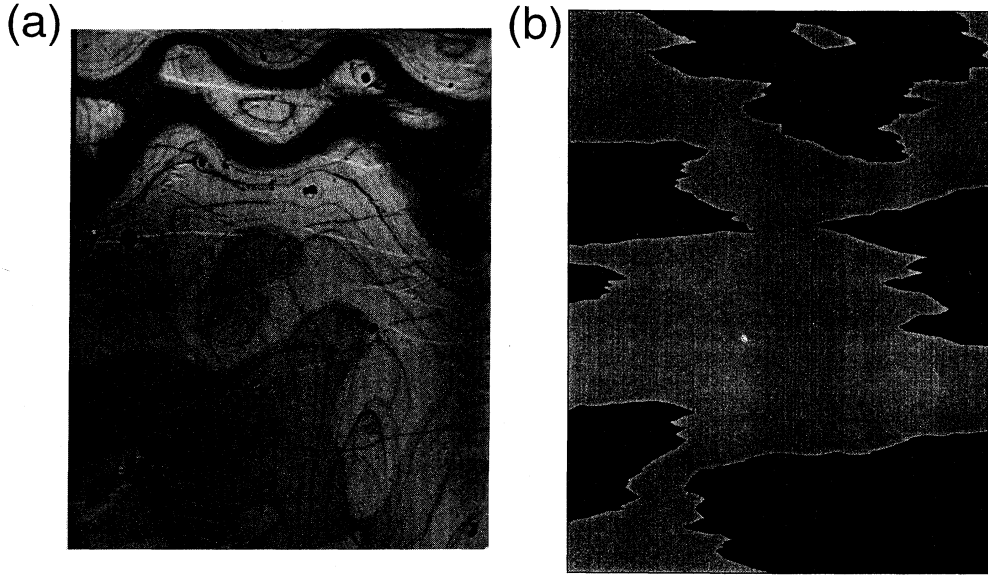


FIG. 8. An example of a Fresnel image taken by Lorentz microscopy (a) and the deduced orientations of the magnetization over this observed region (b).

From Fig. 9, the overall microscopic magnetization reversal process for fields close to the $\langle 110 \rangle$ direction can now be explained. These results should be compared with Fig. 5 which shows the magnetization reversal process deduced from the MOKE measurements. The reversal sequence proceeds as follows. As the field strength is reduced from a high value along the $[110]$ direction to zero, the magnetization undergoes coherent rotation from close to the $[110]$ direction and moves toward the nearest easy axis, the $[100]$ direction in this case. No domain walls are observed at this point, Fig. 9(a),

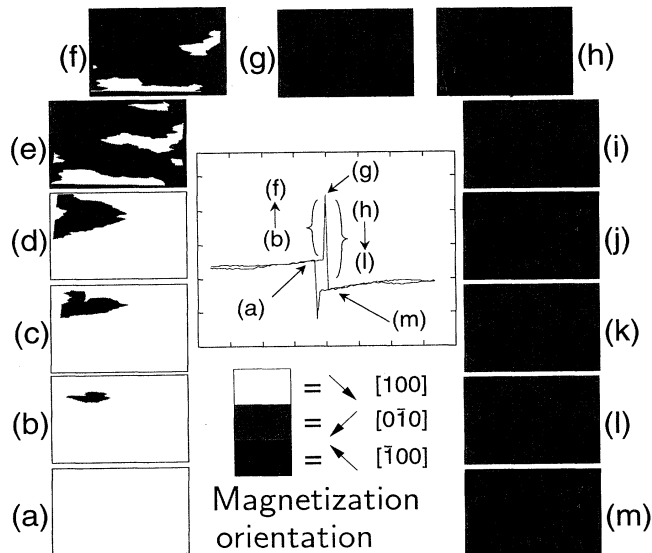


FIG. 9. A sequence of magnetization orientations deduced from Lorentz microscopy Fresnel images during the reversal process in a film with $r=0.16$ for a field applied close to the hard axis, showing the two-jump reversal mechanism microscopically.

confirming that the sample is in an almost single-domain state during the coherent-rotation process, corresponding precisely to the observed MOKE results, stage 1 in Fig. 5. Further application of a field of the opposite polarity (namely, one parallel to $[\bar{1}\bar{1}0]$) causes further coherent rotation as the magnetization moves away from the $[100]$ direction until, at the first critical field H_{c2} , almost 90° domain walls are nucleated, Fig. 9(b), and these jump across the specimen, Figs. 9(c)–9(f), introducing domains in which the magnetization is oriented close to $[0\bar{1}0]$, the easy direction that is now nearer to that of the reversed applied field. Increasing the field strength by only several oersteds ($\sim 0.2H_{c2}$) allows almost $[0\bar{1}0]$ -oriented domains to grow through Barkhausen-like jumps, the jump distance being of the order of a few tens of micrometers as judged directly from observations on the Lorentz TEM screen. This part of the reversal process corresponds to stage 2 in Fig. 5, the first jump seen in the MOKE loop. When it is complete the whole of the film is once again uniformly magnetized as shown in Fig. 9(g) but the direction of magnetization has changed from being close to $[100]$ to lying close to $[0\bar{1}0]$.

As the reverse field strength is increased further, the uniform magnetization vector shown in Fig. 9(g) moves slightly away from the $[0\bar{1}0]$ direction towards that of the applied field, stage 3 in Fig. 5. Increasing the reverse field strength to the second critical value H_{c1} leads to the nucleation and expansion of new domains in which the magnetization is now oriented close to the $[\bar{1}00]$ direction, Figs. 9(h)–9(m). This corresponds to stage 4 in Fig. 5, the second jump seen in the MOKE loop. It is important to note that the domain walls at this stage oriented almost along the $[\bar{1}10]$ direction rather than the $[110]$ direction as was the case in the first switching stage [Figs. 9(b)–9(f)], confirming the two jumps of almost 90° in the magnetization. These new domains grow quickly again through Barkhausen-like jumps until the film reaches the third single-domain state in which the magnetization is uniformly oriented close to $[\bar{1}00]$, Fig. 9(m). Increasing

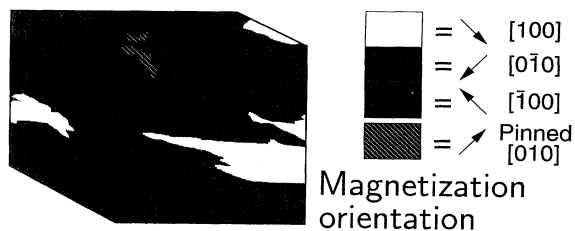


FIG. 10. The magnetization orientations deduced from a Lorentz microscopy Fresnel image for a film with $r=0.16$ for a field applied close to the easy axis, showing the three magnetization orientations observed in the intermediate state during reversal.

the reverse field further leads to a coherent rotation of magnetization away from the $[\bar{1}00]$ direction towards that of the applied field until the film is saturated, stage 5 in Fig. 5. Repetition of the field cycle described above showed that the fields at which walls appeared and disappeared were highly reproducible, but that they occurred at different positions on the sample. Defects do limit the size of the domains in some places but this only “perturbs” the behavior.

When the field direction gets to within 5° of an easy axis we find that the intermediate single-domain state [Fig. 9(g)] no longer appears, and instead a state occurs in which all three domain orientations are found, Fig. 10. This is caused by the “merging” of the two jumps into one near-continuous 180° reversal of the magnetization. Thus the single jump observed macroscopically in the MOKE loops is seen to correspond to a microscopic two-jump process as the magnetization reverses. Note that an additional domain orientation occurs (striped pattern in Fig. 10) due to a strong pinning center associated with a defect. This domain is present even at the largest available field used in the microscope.

V. SUMMARY

We have studied the switching behavior of Fe/GaAs samples for various values of uniaxial and cubic anisotropy constants using in-plane MOKE magnetometry.

Coherent-rotation calculations show that the switching mechanism depends on the angle of the applied field in the plane of the films as well as the ratio of uniaxial and cubic anisotropies. In general, the observed switching behavior agrees well with the switching mechanism predicted by the calculations and previously observed by others, and we were also able to distinguish between two different two-jump switching mechanisms. However, it was found that in some cases domain-wall sweeping mechanisms. However, it was found that in some cases domain-wall sweeping caused two-jump switching where one-jump switching is expected from the calculations, suggesting that further analysis of the reversal process is required to gain an understanding of the switching field values. It was found that the anisotropy ratio could be accurately determined from the MOKE data by determining the angles at which the magnetization switches between a clockwise or anticlockwise motion. A simple analytical expression for this angle was given, and the experimental results for the anisotropy ratio determined from MOKE agreed well with that found from BLS measurements.

Lorentz microscopy results confirm that the sample behaves almost as a single domain, except very close to the regions where a jump is observed during the macroscopic magnetization reversal. During these jumps the Lorentz images reveal that the reversal takes place by domain-wall motion. Also, when the field is applied close to the easy axis, the single jump observed by MOKE in the macroscopic magnetization reversal is actually shown to be a two-step process microscopically. Since the sample behaves almost as a single domain and the switching process is controllable, this behavior is of interest for device applications.

ACKNOWLEDGMENTS

The financial support of the EPSRC, the Toshiba Corporation, and the Newton Trust, Cambridge for this work is gratefully acknowledged. M.G. would like to thank the EC for financial support. S.J.G. would like to thank the DRA, U.K. for support. E.A. would like to thank the Commonwealth Scholarship Commission, U.K.

- ¹J. M. Florczak and E. D. Dahlberg, *J. Appl. Phys.* **67**, 7520 (1990).
- ²J. M. Florczak and E. D. Dahlberg, *Phys. Rev. B* **44**, 9338 (1991).
- ³J. M. Florczak and E. D. Dahlberg, *J. Magn. Magn. Mater.* **104**, 399 (1992).
- ⁴J. J. Krebs, B. T. Jonker, and G. A. Prinz, *J. Appl. Phys.* **61**, 2596 (1987).
- ⁵C. Daboo, R. J. Hicken, D. E. P. Eley, M. Gester, S. J. Gray, A. J. R. Ives, and J. A. C. Bland, *J. Appl. Phys.* **75**, 5586 (1994).
- ⁶E. Gu, J. A. C. Bland, C. Daboo, M. Gester, L. M. Brown, R.

Ploessl, and J. N. Chapman, *Phys. Rev. B* **51**, 3596 (1995).

⁷M. Gester, C. Daboo, S. J. Gray, R. J. Hicken, E. Gu, and J. A. C. Bland (unpublished).

⁸K. B. Hathaway and G. A. Prinz, *Phys. Rev. Lett.* **47**, 1761 (1981).

⁹F. J. Rachford, M. Rubinstein, and G. A. Prinz, *J. Appl. Phys.* **63**, 4291 (1988).

¹⁰E. C. Stoner and E. P. Wohlfarth, *Philos. Trans. R. Soc. A* **240**, 599 (1948).

¹¹C. Daboo, J. A. C. Bland, R. J. Hicken, A. J. R. Ives, M. J. Baird, and M. J. Walker, *Phys. Rev. B* **47**, 11 852 (1993).

¹²J. Yuan, E. Gu, M. Gester, J. A. C. Bland, and L. M. Brown,

- J. Appl. Phys. **75**, 6501 (1993).
- ¹³R. J. Hicken, D. E. P. Eley, M. Gester, S. J. Gray, C. Daboo, A. J. R. Ives, and J. A. C. Bland, *J. Magn. Magn. Mater.* **145**, 278 (1995).
- ¹⁴B. Diény, J. P. Gavigan, and J. P. Rebouillat, *J. Phys. Condens. Matter* **2**, 159 (1990).
- ¹⁵C. Daboo, J. A. C. Bland, R. J. Hicken, A. J. R. Ives, M. J. Baird, and M. J. Walker, *J. Appl. Phys.* **73**, 6368 (1993).
- ¹⁶J. N. Chapman, S. McVitie, and S. J. Hefferman, *J. Appl. Phys.* **69**, 6078 (1991).

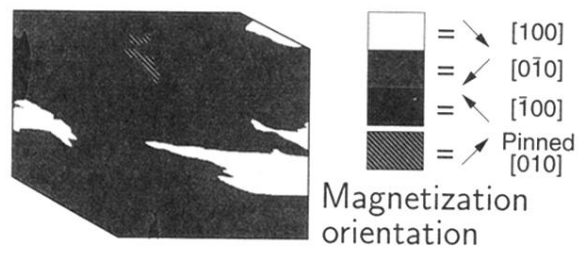


FIG. 10. The magnetization orientations deduced from a Lorentz microscopy Fresnel image for a film with $r=0.16$ for a field applied close to the easy axis, showing the three magnetization orientations observed in the intermediate state during reversal.

(a)



(b)

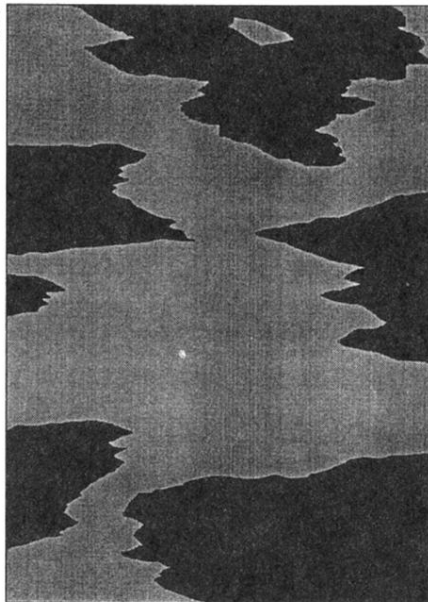


FIG. 8. An example of a Fresnel image taken by Lorentz microscopy (a) and the deduced orientations of the magnetization over this observed region (b).

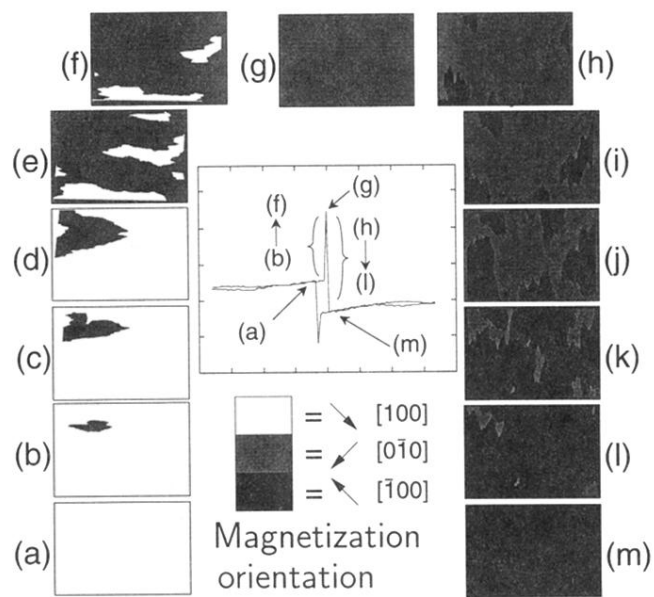


FIG. 9. A sequence of magnetization orientations deduced from Lorentz microscopy Fresnel images during the reversal process in a film with $r=0.16$ for a field applied close to the hard axis, showing the two-jump reversal mechanism microscopically.